The Trilemma Between Accuracy, Timeliness and Smoothness in Real-Time Signal Extraction

Marc Wildi, Tucker McElroy

February 28, 2018

Abstract

The evaluation of economic data and monitoring of the economy is often concerned with an assessment of mid- and long-term dynamics of time series (trend and/or cycle). Frequently, one is interested in the most recent estimate of a target signal, a so-called real-time estimate. Unfortunately, real-time signal extraction is a difficult estimation problem that involves linear combinations of possibly infinitely many multi-step ahead forecasts of a series. We here address performances of real-time designs by proposing a generic Direct Filter Approach. We decompose the ordinary Mean Squared Error into Accuracy, Timeliness and Smoothness error components, and we propose a new tradeoff between these competing terms, the so-called ATS-trilemma. With this formalism, we are able to derive a general class of optimization criteria that allow the user to address specific research priorities, in terms of the Accuracy, Timeliness and Smoothness properties of the corresponding concurrent filter. We illustrate the new methods through simulations, and present an application to Indian Industrial Production data.

1 Introduction

The evaluation of economic data and monitoring of the economy is often concerned with an assessment of mid- and long-term dynamics of time series (trend and/or cycle). While this is acknowledged as an important task for developed nations, for developing countries the assessment of such dynamics is arguably even more crucial and challenging, given the more volatile nature of such data. A broad range of techniques are available to the analyst: ARIMA-based approaches (e.g., TRAMO-SEATS (Maravall and Caparello, 2004)), State-Space methods (e.g., STAMP (Koopman, Harvey, Doornik, Shepherd (2000)), and classic filters (e.g., Hodrick-Prescott (HP) or Cristiano-Fitzgerald (CF); see Hodrick and Prescott (1997) and Cristiano and Fitzgerald (2003)). Frequently, one is interested in the most recent estimate of a target signal, which depends on only present and past data through a concurrent filter, and is referred to as a real-time estimate. Unfortunately, performances of real-time estimates generally differ from performances of historical estimates (based upon symmetric filters, also called smoothers) because the former cannot rely on future data, i.e., concurrent filters are asymmetric. We here address performances of real-time designs (although the method can be easily extended to smoothing) by proposing a generalization of the Direct Filter Approach (DFA) first introduced in Wildi (2005). The new idea of this paper is that real-time estimates can be constrained to have desirable properties – such as increased smoothness and timeliness – by direct design of the corresponding concurrent filter.

In order to impose these desirable properties on a filter, we proceed by decomposing the signal extraction mean squared error (MSE) into components that correspond to the key properties of a filter. It is well-known (Priestley, 1981) that any linear filter is characterized by its frequency response function (frf), i.e., the Discrete Fourier Transform (DFT) of its filter coefficients, and the frf can be decomposed in terms of a gain function and a phase function. The former governs the smoothness of filter estimates, describing the so-called pass-band and stop-band, whereas the latter governs the timeliness of the filter, controlling the temporal advance or retardation of underlying

harmonics. Here, we make a novel connection of these concepts to the signal extraction MSE. We decompose the ordinary MSE into Accuracy, Timeliness and Smoothness error components, and we propose a new tradeoff between these competing terms, the so-called ATS-trilemma. In a way this is analogous to the bias-variance dilemma that arises from the classical decomposition of a parameter estimator's MSE but it is a richer two-dimensional tradeoff between three competing terms which address signal extraction, explicitly.

With this formalism, we are able to derive a general class of optimization criteria that allow the user to address specific research priorities, in terms of the Accuracy, Timeliness and Smoothness properties of the corresponding concurrent filter. We call such a criterion a "customization". Although customization for real-time signal extraction can be achieved via other methodologies, we argue that our particular decomposition of MSE offers the most direct and compelling connection between parameters and the corresponding characteristics of a concurrent filter. For example, in a model-based framework (e.g., TRAMO-SEATS or STAMP) one could adjust model orders and/or model parameters to achieve modifications to smoothness (e.g., increase the integration order for the trend to obtain a smoother real-time trend), but the connection of such adjustments to the phase function of the concurrent filter arising from such models is much harder to discern; moreover, knowing the phase function alone does not provide information about its impact on MSE – and one is ultimately concerned about signal extraction error. If instead one advocates using an asymmetric version of a popular nonparametric filter, such as the HP, CF, or ideal low-pass filter, there are few parameters available to adjust the phase function, and the story is much the same as in the model-based framework. So while we acknowledge that other methodologies provide a connection between parameters and vague notions of smoothness and phase, our contribution here is to make these connections mathematically explicit through the ATS decomposition. The ATS decomposition can in fact be used to analyze and customize a model-based concurrent filter, or a nonparametric concurrent filter; we advocate working with a richer class of concurrent filters, that allow for more flexibility in terms of gain and phase functions, than is typically possible with model-based or nonparametric approaches.

If one were to weight squared bias and variance by some convex combination – where equal weights correspond to the estimator's MSE – one could emphasize either aspect, depending upon user priorities. Such a customization results in a one-dimensional space – or curve – of criteria, the classical MSE being but the central point. Similarly, real-time signal extraction customization results in a two-dimensional space – or triangle – of criteria, wherein the MSE lies in the center, and the vertices correspond to exclusive emphasis on either Accuracy, Timeliness, or Smoothness. Thus, traditional approaches (such as those discussed above) can be replicated perfectly by DFA, and can also be customized. Interestingly, the two-dimensional tradeoff collapses to a bipolar dilemma in a classic one- or multi-step ahead forecast perspective, which we demonstrate below (essentially because the notions of pass-band and stop-band are irrelevant in forecasting problems). The key facet here is that MSE can be decomposed into a summation of constituent error measures that correspond to useful quantities of interest. Just as with a classical estimator, where it is useful to examine both its squared bias and its variance – described heuristically as accuracy and precision respectively – here in the context of signal extraction it is useful to decompose MSE into the three components of Accuracy, Timeliness, and Smoothness. As in nonparametric density estimation, where altering the bandwidth can decrease bias at the expense of higher variance, or vice versa, so here an improvement of one of the ATS components typically entails a deterioration in one or both of the other components.

The main concepts are introduced in Section 2. We then replicate and customize a simple generic model-based filter in Section 3, to demonstrate that DFA includes the classical approaches, while being more flexible. We propose classic time-domain performance measures, namely peak-correlation (for Timeliness) and curvature (mean square second-order differences for Smoothness) and illustrate that the customized design can outperform model-based filters in both aspects simultaneously, out-of-sample. Due to space limitations we here restrict the exposition to univariate approaches, though customization and the underlying trilemma readily extend to multivariate approaches; this is currently being investigated by the authors. Section 4 eschews the model-based framework, providing nonparametric results. Section 5 provides an application to nowcasting In-

dian Industrial Production data, with the finding of positive growth starting in 2015, based upon a customized filter. Section 6 summarizes our findings.

2 ATS-Trilemma and Customization

Here we introduce the mathematical concepts needed; some of this material can be found in Wildi and McElroy (2016), but Section 2.3 here is novel, and exposits the main thesis of this paper.

2.1 Target

Let $\{x_t\}$ be our time series data. We assume that the target (signal) $\{y_t\}$ is specified by the output of a (possibly bi-infinite) filter applied to x_t

$$y_t = \sum_{k=-\infty}^{\infty} \gamma_k x_{t-k}, \tag{1}$$

and we denote by $\Gamma(\omega) = \sum_{k=-\infty}^{\infty} \gamma_k \exp(-ik\omega)$ the frf of the filter. This specification is completely general, such that we could account for model-based targets (based on ARIMA or State Space models), nonparametric filters (HP, CF, or Henderson (1916)), or "ideal" low-pass and band-pass filters such as

$$\Gamma(\omega; \eta_1, \eta_2) = 1_{[\eta_1, \eta_2]}(|\omega|) \tag{2}$$

where $0 \leq \eta_1 < \eta_2$ and with the convention that $\Gamma(\omega; \eta_1, \eta_2)$ is a low-pass if $\eta_1 = 0$. The ideal low-pass and band-pass filter are symmetric, with $\gamma_k = (\sin[\eta_2 k] - \sin[\eta_1 k])/(\pi k)$ for $k \geq 1$ and $\gamma_0 = (\eta_2 - \eta_1)/\pi$. Typically, signal extraction targets are symmetric ($\gamma_k = \gamma_{-k}$) but our definition (1) allows for a general specification. As an example, h-step ahead forecasting would be obtained by setting $\gamma_k = 1_{\{k=-h\}}$. The resulting transfer function $\Gamma(\omega) = \exp(ih\omega)$ would be an anticipative allpass filter.

2.2 Mean Square Paradigm

We seek a concurrent filter, called $\widehat{\Gamma}$ (because it is a concurrent approximation to Γ) of a given length $L > 0$. Let $\widehat{\Gamma}(B) = \sum_{k=0}^{L-1} b_k B^k$, expressed in terms of the backshift operator B. We seek filter coefficients $\{b_k\}$ such that the finite sample estimate

$$\widehat{y}_t := \sum_{k=0}^{L-1} b_k x_{t-k} \tag{3}$$

is as close as possible to y_t in mean square, i.e., we need to solve

$$\arg\min_{\mathbf{b}} E\left[(y_t - \widehat{y}_t)^2\right], \tag{4}$$

where $\mathbf{b} = [b_0, b_1, \cdots, b_{L-1}]'$. We could restrict $\widehat{\Gamma}(B)$ to filters that arise as the concurrent filter of a particular model (see Bell and Martin (2004) for the formula of a concurrent filter as a function of signal and noise models), in which case there is a model parameter θ such that $\mathbf{b}$ is a function of θ. Typically, θ has dimension lower than L, which may be fairly large (e.g., $L = 100$). Alternatively, $\widehat{\Gamma}(B)$ may be a concurrent version of a nonparametric filter, such as the Henderson trend filter. Here too $\mathbf{b}$ is a function of parameters θ that govern smoothing. In the Henderson case, θ is scalar and discrete, corresponding to the available (discrete) orders of Henderson filters. For the HP, θ corresponds to a scalar smoothing parameter. We also consider the case that $\widehat{\Gamma}(B)$ is not a function of an underlying parameter, but involves the full class of order L moving average filters; see Wildi and McElroy (2016).

For simplicity of exposition we now assume that $\{x_t\}$ is a weakly stationary process with a continuous spectral density h (the DFT of the autocovariance function) such that

$$E\left[(y_t - \widehat{y}_t)^2\right] = \frac{1}{2\pi}\int_{-\pi}^{\pi} |\Gamma(\omega) - \widehat{\Gamma}(\omega)|^2 h(\omega) d\omega. \tag{5}$$

This follows from the fact that $y_t - \widehat{y}_t = (\Gamma(B) - \widehat{\Gamma}(B))x_t$, which has spectrum $|\Gamma(e^{-i\omega}) - \widehat{\Gamma}(e^{-i\omega})|^2 h(\omega)$; see Brockwell and Davis (1991). Generalizations to non-stationary integrated processes are proposed in Wildi (2005) and Wildi and McElroy (2016)[1]. Replication of traditional model-based filter-designs is obtained by plugging the corresponding target signal $\Gamma(\omega)$ and the corresponding spectral density h (pseudo-spectral density in the case of integrated processes – see Bell and Hillmer (1984) for discussion) into (5).

2.3 Accuracy, Timeliness and Smoothness Components

Consider the following identity

$$\begin{aligned} |\Gamma(\omega) - \widehat{\Gamma}(\omega)|^2 &= A(\omega)^2 + \widehat{A}(\omega)^2 - 2A(\omega)\widehat{A}(\omega)\cos\left(\Phi(\omega) - \widehat{\Phi}(\omega)\right) \\ &= (A(\omega) - \widehat{A}(\omega))^2 \\ &\quad + 4A(\omega)\widehat{A}(\omega)\sin^2\left(\frac{\Phi(\omega) - \widehat{\Phi}(\omega)}{2}\right) \end{aligned} \tag{6}$$

where $A(\omega) = |\Gamma(\omega)|$, $\widehat{A}(\omega) = |\widehat{\Gamma}(\omega)|$ are amplitude functions and $\Phi(\omega) = Arg(\Gamma(\omega))$, $\widehat{\Phi}(\omega) = Arg(\widehat{\Gamma}(\omega))$ are phase functions of the filters involved. In the case of typical signal extraction problems, where Γ is a symmetric filter, the phase of the target vanishes, i.e., $\Phi(\omega) = 0$. In the case of h-step ahead forecasting, the phase becomes $\Phi(\omega) = h\omega$. We now plug (6) into (5), and obtain the following decomposition of the signal extraction MSE:

$$\begin{aligned} \int_{-\pi}^{\pi} \left|\Gamma(\omega) - \widehat{\Gamma}(\omega)\right|^2 h(\omega)d\omega &= \int_{-\pi}^{\pi} (A(\omega) - \widehat{A}(\omega))^2 h(\omega)d\omega \\ &\quad + 4\int_{-\pi}^{\pi} A(\omega)\widehat{A}(\omega))\sin^2\left(\frac{\Phi(\omega) - \widehat{\Phi}(\omega)}{2}\right) h(\omega)d\omega. \end{aligned}$$

In the case of signal extraction we can specify pass-bands and stop-bands of a filter by

$$\begin{aligned} \text{pass-band} &= \{\omega | A(\omega) \geq 0.5\} \\ \text{stop-band} &= [-\pi, \pi] \setminus \text{pass-band}. \end{aligned}$$

The original MSE can then be decomposed additively into the following four terms:

$$\text{Accuracy} := \int_{\text{pass-band}} (A(\omega) - \widehat{A}(\omega))^2 h(\omega)d\omega \tag{7}$$

$$\text{Timeliness} := 4\int_{\text{pass-band}} A(\omega)\widehat{A}(\omega)\sin^2\left(\frac{\Phi(\omega) - \widehat{\Phi}(\omega)}{2}\right) h(\omega)d\omega \tag{8}$$

$$\text{Smoothness} := \int_{\text{stop-band}} (A(\omega) - \widehat{A}(\omega))^2 h(\omega)d\omega \tag{9}$$

$$\text{Residual} := 4\int_{\text{stop-band}} A(\omega)\widehat{A}(\omega)\sin^2\left(\frac{\Phi(\omega) - \widehat{\Phi}(\omega)}{2}\right) h(\omega)d\omega \tag{10}$$

[1] Under suitable filter restrictions, the filter error $y_t - \widehat{y}_t$ is weakly stationary even if $\{x_t\}$ is integrated.

Accuracy measures the contribution to the MSE when the phase (time-shift) and the noise suppression in the stop-band are ignored. This would correspond to the performance of a symmetric filter (no time-shift) with perfect noise suppression, i.e., $\widehat{A} = 0$ in the stop-band, and with the same amplitude as the considered concurrent filter in the pass-band. A corresponding symmetric filter could be easily constructed by inverse Fourier transformation. Smoothness measures the MSE contribution attributable to the leakage of the concurrent filter in the stop-band, corresponding to undesirable high-frequency noise. This quantity is linked to the well-known time-domain "curvature'" measure described in Section 3.2. Timeliness measures the MSE contribution generated by the time-shift. It is linked to the time-domain "peak-correlation" concept described in Section 3.2. Finally, the Residual is that part of the MSE which is not attributable to any of the above error components. Since the product $A(\omega)\widehat{A}(\omega)$ is small in the stop-band (possibly vanishing, as in the case of the ideal low-pass) the Residual is generally negligible. From a slightly different perspective, user priorities are rarely concerned about time-shift properties of components in the stop-band, which ought to be damped or eliminated anyways. For the sake of simplicity we henceforth focus on the ideal low-pass target, wherein the Residual vanishes completely.

2.4 Signal Extraction ATS-Trilemma and Customization

The best MSE concurrent filter provides a benchmark, which however can be beaten by other filters according to the facets of Accuracy, Smoothness, or Timeliness. It is not possible for another filter to improve upon the benchmark according to all three of these facets – because then such a filter would have better overall MSE (omitting the Residual in this discussion) – but we may possibly improve two aspects simultaneously, at the expense of the third. For example, it can be shown that we can always improve Accuracy and Smoothness, at the expense of increased phase delay. The MSE criterion balances these terms, being the straight summation of (7), (8), and (9); weighting these terms unevenly will enforce different emphases, giving rise to quite different concurrent filters.

More formally, the MSE can be easily generalized to provide a customized measure by assigning weights to the terms of its ATS decomposition:

$$\mathcal{M}(\vartheta_1, \vartheta_2) = \vartheta_1 \,\text{Timeliness} + \vartheta_2 \,\text{Smoothness} + (1 - \vartheta_1 - \vartheta_2)\,\text{Accuracy}. \tag{11}$$

The parameters $\vartheta_1, \vartheta_2 \in [0, 1]$ (such that $\vartheta_1 + \vartheta_2 \leq 1$) allow one to assign priorities to single or pairwise combinations of MSE error terms: the resulting two-dimensional tradeoff is called the ATS-trilemma, and the optimization paradigm (11) is called a customized criterion. Plotting $\mathcal{M}(\vartheta_1, \vartheta_2)$ over the ϑ_1- and ϑ_2-axes yields a surface defined over a triangle with vertices $(0, 0)$, $(1, 0)$, and $(0, 1)$, which we call the "customization triangle." The user is free to navigate on the customization triangle according to specific research priorities. The ordinary MSE criterion (referred to as the "default" henceforth) is obtained by setting $\vartheta_1 = \vartheta_2 = 1/3$, whereas the edges correspond to the complete absence of one of the A,T, S terms, and the vertices emphasize one component to the exclusion of all others.[2]

The criterion (11) is also impacted by the choice of pass-band; altering the pass-band from the definition $\{\omega | A(\omega) \geq 0.5\}$ indeed changes the corresponding values of the Accuracy, Timeliness, and Smoothness terms, and in turn affects the resulting customized filter. For instance, allowing the pass-band to encompass a greater range will demand that our customized filter be timely (say, if $\vartheta_1 > 0$) across a greater range of frequencies.

The schematic criterion (11) could be usefully extended by introducing non-negative weighting functions $W_1(\omega)$, $W_2(\omega)$ to the Timeliness and Smoothness terms:

$$\text{Timeliness} = 4 \int_{\text{pass-band}} A(\omega)\widehat{A}(\omega) \sin^2 \left(\frac{\Phi(\omega) - \widehat{\Phi}(\omega)}{2} \right) W_1(\omega) h(\omega) d\omega \tag{12}$$

$$\text{Smoothness} = \int_{\text{stop-band}} (A(\omega) - \widehat{A}(\omega))^2 \, W_2(\omega) h(\omega) d\omega \tag{13}$$

[2]By fixing the length L of the concurrent filters, each of the A,T, and S terms will be finite, ensuring that no numerical problems result when customizing on the triangle's edges.

These weighting functions can be viewed as extensions of the constant weights ϑ_1 and ϑ_2 appearing in 11, which weight Timeliness and Smoothness, respectively. For example, we may wish to de-emphasize higher frequencies in the Smoothness term, in order to avoid the incidence of false turning points in the real-time signal; this could be accomplished by letting $W_2(\omega)$ take larger values for ω in the stop-band. While there is no best choice for such weighting functions, their design should correspond to the priorities of each user; we provide an example in the empirical section below.

2.5 Forecast AT-Dilemma

The above trilemma was obtained by assuming that the target filter Γ discriminates components into pass- and stop-bands. In contrast, h-step ahead forecasting is concerned with the approximation of an anticipative allpass filter. Since the stop-band is non-existant, the Smoothness and Residual error components vanish and the above trilemma collapses into a forecasting dilemma:

$$\mathcal{M}(\vartheta_1) = \vartheta_1 \,\text{Timeliness} + (1-\vartheta_1)\,\text{Accuracy}$$

This function $\mathcal{M}(\vartheta_1)$ could be plotted against $\vartheta_1 \in [0,1]$, yielding a curve. While this paradigm is sufficient to address all-pass filtering problems, such as multi-step ahead forecasting, it cannot emphasize Smoothness, and hence is not sufficient for more general real-time estimation problems – for which (11) is preferred.

2.6 Spectrum, Signal and Customization Interfaces

The proposed method can replicate and customize traditional (ARIMA or State-Space) model-based approaches as well as classic filter designs (HP, CF, Henderson), by plugging the corresponding spectral densities as well as the target signals into (11). We could combine these in any order: as an example, we could target a HP filter by supplying a model-based spectral density. Moreover, we could use alternative spectral estimates (e.g., nonparametric) or targets: the resulting spectrum- and signal-interfaces allow for a flexible implementation of general forecasting and signal extraction problems. Examples of hybrid real-time trend extraction and seasonal adjustment problems are provided in Wildi and McElroy (2016).

The customization interface (11) allows one to emphasize particular filter characteristics, so as to align with research priorities. For instance, one can set the pass-band and stop-band according to which frequencies are of greatest interest for the application. One can also use the criterion (11) to obtain customized filters subject to some constraint (this would be accomplished by minimizing $\mathcal{M}(\vartheta_1, \vartheta_2)$ subject to a hard constraint on the filter coefficients $\widehat{\Gamma}$), e.g., constraining Timeliness to equal some specified value, and searching for a real-time filter that has the best possible Accuracy and Smoothness given this condition.

3 Replicating and Customizing a Model-Based Approach

3.1 Empirical Design

We here propose a simple simulation framework based on an ideal low-pass target with cutoff $\pi/12$ given by $\Gamma(\omega; 0, \pi/12)$ (which implies that $\gamma_k = \frac{\sin(k\pi/12)}{k\pi}$ for $k \neq 0$ and $\gamma_0 = \frac{1}{12}$) and an AR(1) data generating process (DGP) $\{x_t\}$ satisfying

$$x_t \;=\; a x_{t-1} + \epsilon_t \tag{14}$$

and $\{\epsilon_t\}$ a white noise process. Our framework is pertinent to real-time economic indicators: log-returns of macro-data[3] can be fitted more or less satisfactorily by benchmark AR(1) models, and users are typically interested in inferring business cycle or trend dynamics from such a design.

[3]Industrial production, employment or income, as proposed and used by the NBER.

Our framework is hybrid in the sense that we target a non model-based signal (the ideal trend) based upon a model of the DGP. Our artificial framework is deliberately over-simplified in order to highlight the salient features of the ATS-trilemma.

As mentioned above, weighting functions can be introduced to the Timeliness (12) and Smoothness (13) terms. Here (letting $\pi/12$ be the cutoff of the target signal) we adopt weighting functions

$$\left.\begin{array}{rcl} W_1(\omega;\lambda) & = & 1+\lambda \\ W_2(\omega;\eta) & = & (1+|\omega|-\pi/12)^{\eta} \end{array}\right\} \tag{15}$$

and utilize criterion (11) with the basic definition of the Accuracy term (7). For $\lambda = \eta = 0$ the equally-weighted criterion (i.e., the MSE benchmark) is obtained; $\lambda > 0$ emphasizes Timeliness uniformly across frequencies (and is equivalent to increasing ϑ_1), whereas adopting $\eta > 0$ highlights Smoothness by further penalizing amplitude discrepancies in the stop-band. We can balance the impact of Timeliness and Smoothness by taking moderate values of both λ and η – by experimentation we have found found that $\lambda = 30$ and $\eta = .5$ are adequate for this purpose.

3.2 Performance Measures

We rely on the following time-domain measures for assessing out-of-sample performances of our concurrent filter designs:

$$\text{Curvature} \quad := \quad \frac{E\left[\left((1-B)^2\widehat{y}_t\right)^2\right]}{\text{var}(\widehat{y}_t)} \tag{16}$$

$$\text{Peak-Correlation} \quad := \quad \text{Arg}\left(\max_j(cor(y_t,\widehat{y}_{t+j}))\right) \tag{17}$$

$$\text{Sample-MSE} \quad := \quad E\left((y_t-\widehat{y}_t)^2\right) \tag{18}$$

Mean square second-order differences emphasize the geometric curvature of a time series; smaller Curvature leads to a smoother appearance of a filtered series (e.g., having less noisy ripples). The proposed measure is normalized in order to immunize against scaling effects. Note that we are not primarily interested in the magnitude of the correlations in (17), but in the integer j_0 at which the correlation between the target y_t and the shifted (real-time) estimate $\widehat{y}_{t+j_0}$ is maximized. The latter is called leading, coincident or lagging depending on j_0 being negative, zero or positive respectively. The Sample-MSE is computed in order to assess the overall loss in mean square performances entailed by customization.

Since expectations are unknown, we shall report sample distributions (box-plots) of the above performance measures, distinguishing in- and out-of-sample periods. In particular we shall benchmark four empirical filters – three customized and one default (i.e., taking $\lambda = \eta = 0$ and $\vartheta_1 = \vartheta_2 = 1/3$ in (11)) – against the best possible filter (assuming knowledge of the true AR(1) DGP).

3.3 A Generic Model-Based Approach

Given a sample $x_1, ..., x_T$ of $\{x_t\}$, the generic model-based approach to obtaining a concurrent filter consists in forecasting and backcasting missing data in the target specification. Letting $t = T$ in (1) we obtain

$$y_T = \sum_{k=-\infty}^{-1}\gamma_k x_{T-k} + \sum_{k=0}^{T-1}\gamma_k x_{T-k} + \sum_{k=T}^{\infty}\gamma_k x_{T-k},$$

which partitions the target into future observations, available data, and past observations. The future and past sections are unobserved, so the corresponding x_{T-k} must be replaced by a projection $\widehat{x}_{T-k}$, which is a forecast if $k < 0$ and a backcast if $k \geq T$. Assuming the AR(1) model is

correct, we obtain $\widehat{x}_{T-k} = a^{-k}x_T$ for forecasts and $\widehat{x}_{T-k} = a^{k-T+1}x_1$ for backcasts. Substituting these into the expression for y_T, we obtain

$$\begin{aligned}\widehat{y}_T &= \sum_{k=-\infty}^{-1} \gamma_k a^{-k} x_T + \sum_{k=0}^{T-1} \gamma_k x_{T-k} + \sum_{k=T}^{\infty} \gamma_k a^{k-T+1} x_1 \\ &= \left(\sum_{k=0}^{\infty} \gamma_{-k} a^{-k}\right) x_T + \sum_{k=1}^{T-2} \gamma_k x_{T-k} + \left(\sum_{k=0}^{\infty} \gamma_{T-1+k} a^{k}\right) x_1.\end{aligned}$$

Comparing this expression with equation (3) and setting $L = T$, we see that

$$b_0 = \sum_{k=0}^{\infty} \gamma_{-k} a^{-k}, \quad b_{T-1} = \sum_{k=0}^{\infty} \gamma_{T-1+k} a^{k},$$

and $b_k = \gamma_k$ for $1 \leq k \leq T-2$. Clearly for T large, $b_{T-1} \approx 0$. This calculation can be generalized to ARMA processes (Wildi and McElroy (2016)). The formula emphasizes explicitly the forecast paradigm underlying classic model-based approaches.

We now compare the above filter coefficients b_j with those obtained by (11), assuming $\lambda = \eta = 0$ (continuous integrals are substituted by discrete sums). Figure 1 illustrates the outcome for three different DGPs based on $a = -0.9, 0.25, 0.9$ in (14). The middle choice $a = 0.25$ corresponds to an AR(1) model fitted to first differences of the (log-transformed) monthly industrial production index, estimated on data from January 1990 to February 2016 (the model passes ordinary diagnostic checks). The high value $a = 0.9$ corresponds to a process with greater frequency content at the low frequencies, whereas $a = -0.9$ corresponds to a spectral density that peaks at frequency π, and has low values in the pass-band. These cases, included for illustrative purposes, represent different challenges for the ATS criterion, as the A and T terms will be large and S will be small when $a = 0.9$ (and vice versa when $a = -0.9$). We set $L = T = 120$ so that the filter and sample lengths correspond to ten years of monthly data.

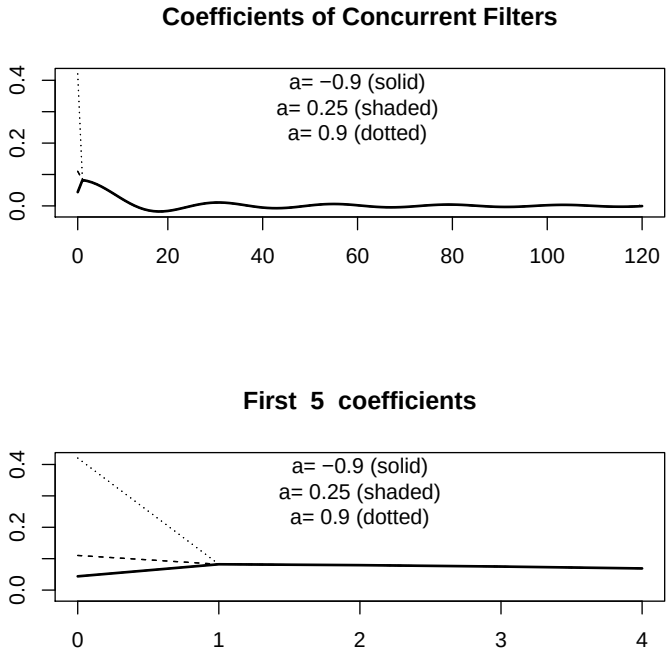

Figure 1: Coefficients of concurrent filters for three different AR(1) processes: model-based coefficients and estimates based on DFA MSE are indistinguishable.

DFA and model-based coefficients virtually overlap for all three DGPs, which confirms the ability of DFA to replicate the model-based approach. The approximation can be improved arbitrarily by selecting a denser frequency-grid, when approximating the continuous integral (5) by a discrete sum.

3.4 Customizing the Model-Based Approach: Known DGP

We first assume knowledge of the true DGP, though this unrealistic assumption is relaxed in section 3.5. This is accomplished by setting $h(\omega) = |1 - ae^{-i\omega}|^{-2}$ in equations (7), (8), (9), and (10). Besides our benchmark filter (solid line in the following figures) corresponding to $\lambda = \eta = 0$ in (15), we propose to compute and analyze three customized designs: a "balanced" filter (dotted line, corresponding to $\lambda = 30$ and $\eta = .5$) that will outperform the benchmark filter in terms of Timeliness *and* Smoothness components, as well as two unbalanced designs, emphasizing more heavily either the facets of Timeliness (large dots, corresponding to $\lambda = 500$ and $\eta = .3$) or Smoothness (solid bold, corresponding to $\lambda = 30$ and $\eta = 1$). Empirical distributions of performance measures will be based on simulated time series of length $T = 1000$ (100 replications).

Amplitude and time-shift functions of all filters for $a = 0.25$ are plotted in Figure 2 (the corresponding Figures **??** and **??** for the DGPs $a = -0.9$ and $a = 0.9$ are to be found in the Supplement).

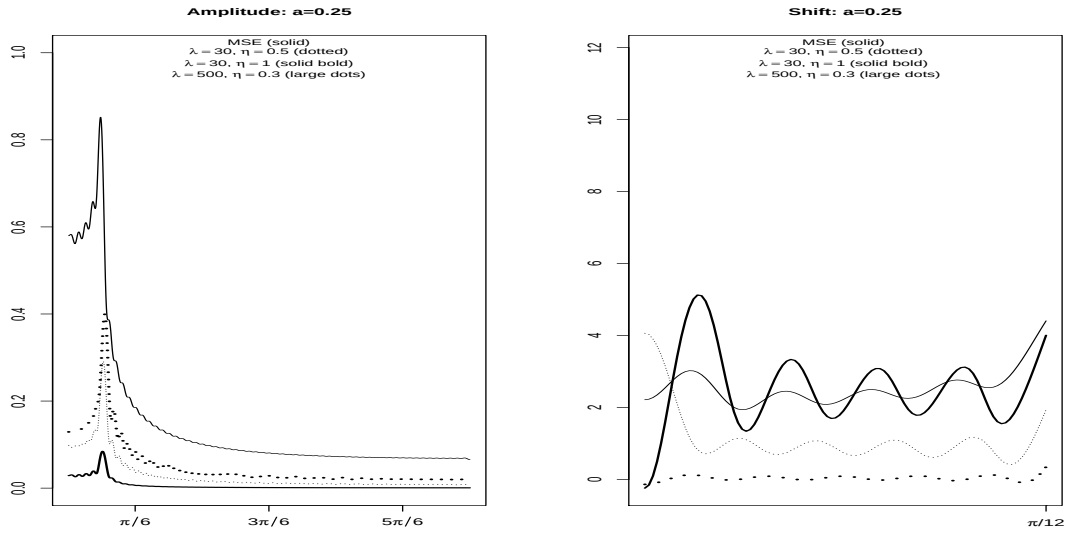

Figure 2: Amplitude and time-shift plots for MBA and customized filters, for AR(1) DGP with $a = 0.25$. Time shift is restricted to the passband of the filters.

Increasing λ tends to decrease the time-shift in the pass-band, as desired. For example, the Timeliness filter (large dots) is a virtually zero-phase concurrent filter. Augmenting η means that the amplitude function in the stop-band is pulled more strongly towards the target (which is zero). Augmenting λ and η simultaneously implies weaker control of the amplitude function in the pass-band by the Accuracy-term.

The empirical distribution of Curvature and Peak-Correlation[4] in Figure 3 confirms the intended effects, namely that both dimensions can be addressed either individually (large dots, solid bold) or simultaneously (dotted) by suitable customization (the other two processes can be seen in Figures **??** and **??** in the Supplement). Stronger customization is accompanied by poorer MSE performances, as expected[5].

[4]The distribution of the Peak-Correlation is concentrated because the time series are long (1000 observations).

[5]Part of the loss in MSE performances is due to zero-shrinkage of customized filter coefficients, and could be avoided by straightforward re-scaling of the filter outputs (these results are not shown here).

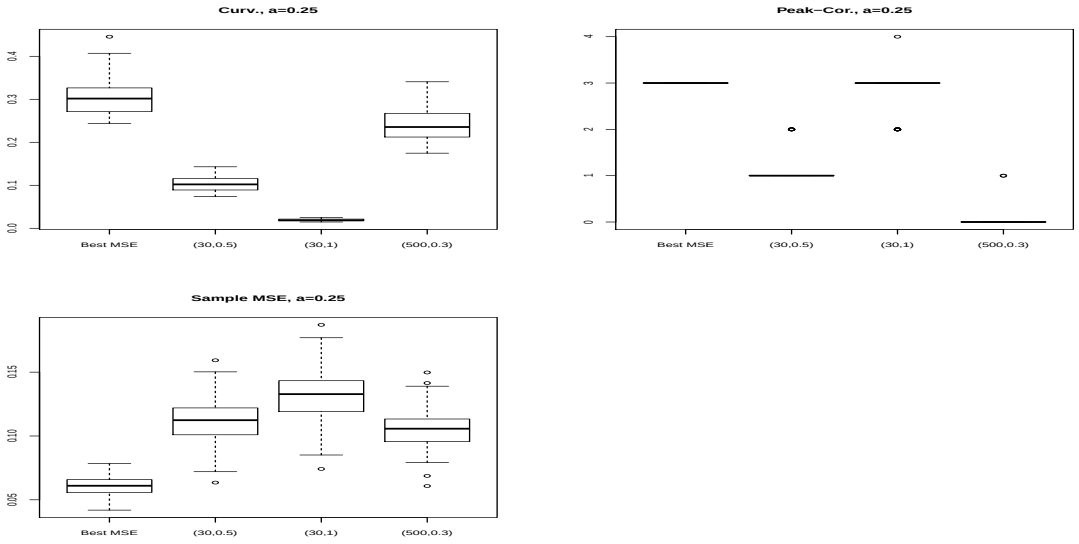

Figure 3: Empirical distributions of Curvature, Peak-Correlation and Sample-MSE, with $a = 0.25$.

Table 1 reports the true MSE as well as the ATS-decomposition of the various designs for $a = 0.25$ (Tables **??** and **??** corresponding to $a = -0.9$ and $a = 0.9$ are to be found in the Supplement). Timeliness and Smoothness components are affected as expected by customization[6].

	Accuracy	Timeliness	Smoothness	Residual	Total MSE
MBA-MSE	0.021153	0.018681	0.024016	0.000000	0.063850
lambda=30, eta=0.5	0.114323	0.000512	0.002403	0.000000	0.117237
lambda=30, eta=1	0.136593	0.000996	0.000151	0.000000	0.137740
lambda=500, eta=0.3	0.104476	0.000008	0.006450	0.000000	0.110934

Table 1: Total MSE and ATS error components for MBA default and customized filters, for AR(1) DGP with $a = 0.25$.

To conclude, we plot filter outputs for a particular realization (the first of the sample) in Figure 4; the other two processes are to be seen in Figures **??** and **??** in the Supplement. A symmetric filter of length 121 is used for reference. All series are standardized for ease of visual inspection.

[6]The shrinkage effect of heavily customized filters (solid bold) distorts these numbers to some extent, such that a direct comparison across filters is less straightforward than with the scale-invariant performance measures in Figures 3, **??** and **??**.

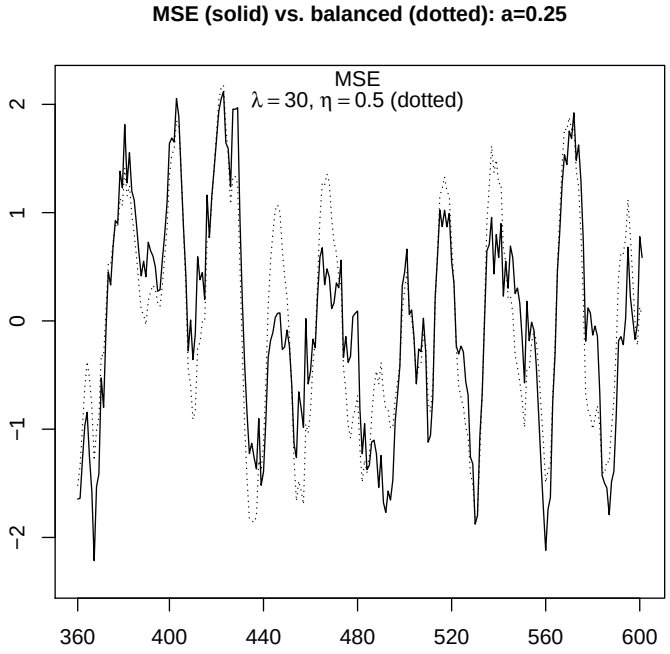

Figure 4: Filter outputs from data simulated from an AR(1) DGP ($a = .25$), comparing historical symmetric (black) estimate versus real-time estimates, using both the benchmark and the customized designs.

Series with smaller Peak-Correlations tend to be shifted leftwards with respect to the benchmark filter outputs (solid), while series with smaller Curvature appear to be smoother, as expected.

3.5 Customizing the Model-Based Approach: Empirical AR(1) Spectrum

The previous results rely on the unrealistic assumption that the true DGP is known. We now analyze empirical spectral estimates based on estimated AR(1) processes, by plugging the estimated autoregressive spectrum in for $h(\omega)$. All estimates rely on samples of length $T = 120$. Out-of-sample performances are computed on samples of length 1000, and empirical distributions of performances rely on 100 replications of this basic setting for each of the above AR(1) processes. In order to avoid identification issues we here assume that the model is known. So for each realization an empirical AR(1) spectrum is obtained from the estimated AR(1) coefficient. In- and out-of-sample empirical distributions of Curvature, Peak-Correlation and Sample-MSE are plotted in Figure 5 for the DGP $a = 0.25$. The other two processes are to be found in the Supplement, in Figures **??** and **??**. Out-of-sample distributions appear more tightly concentrated because the sample lengths are longer (1000 versus 120 in-sample). The balanced design ($\lambda = 30, \eta = 0.5$) clearly outperforms the benchmark filter in terms of smaller Peak-Correlation and Curvature measures, for all three processes, at a cost to MSE performance.

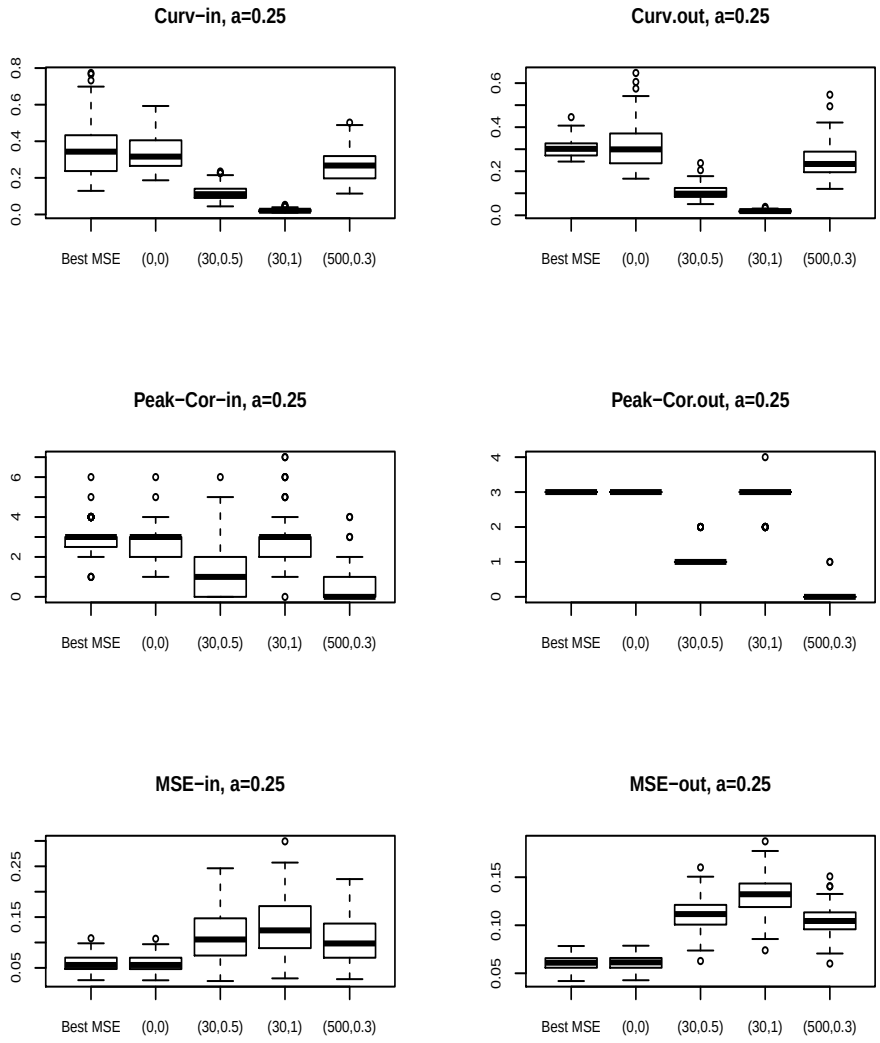

Figure 5: Empirical distributions of Curvature, Peak-Correlation and Sample-MSE based on an estimated AR(1) spectrum, with in-sample results (left plots) and out-of-sample results (right plots) given for $a = 0.25$.

4 Nonparametric Spectrum

In contrast to the previous section, we here ignore a priori knowledge about the true DGP, and use a nonparametric spectral estimate, namely the raw periodogram. We rely on the same empirical setting as in the previous section but we set $L = 24$, and the periodogram is computed on the discrete frequency grid $\omega_k = k2\pi/T$, $k = -T/2, ..., T/2$, where $T = 120$ (ten years of monthly data). The choice of the filter length reflects the maximal duration of components in the stop-band of the target filter (two years). Besides illustrating flexibility, we here also assess overfitting in a richly parametrized framework.

In- and out-of-sample empirical distributions of Curvature, Peak-Correlation and Sample-MSE are plotted in Figure 6 (see also Figures **??** and **??** for the other two processes in the Supplement).

In comparison to the previous AR(1) spectrum out-of-sample MSE performances are only slightly worse. Empirical distributions of Peak-Correlation appear to be more dispersed, while the customization effect appears to be shifted. Peak-Correlations are smaller and Curvatures are larger than those obtained in the previous exercise utilizing an estimated parametric spectrum. The latter effect is due to the fact that the pass-band is short (only six discrete frequency ordinates, including frequency zero) and that the number of freely determined parameters $L = 24$ is comparatively large; therefore, emphasizing time-shift properties in the pass-band (Timeliness) can be addressed more easily than emphasizing amplitude characteristics in the stop-band (Smoothness). Despite the problems of overfitting, we observe that suitably customized filters ($\lambda = 30, \eta = 1$) still outperform the benchmark design in the targeted dimensions, according to out-of-sample criteria. Also, out-of-sample and in-sample performances are remarkably consistent in consideration of the fact that $L = 24$ coefficients are estimated in samples of length $T = 120$.

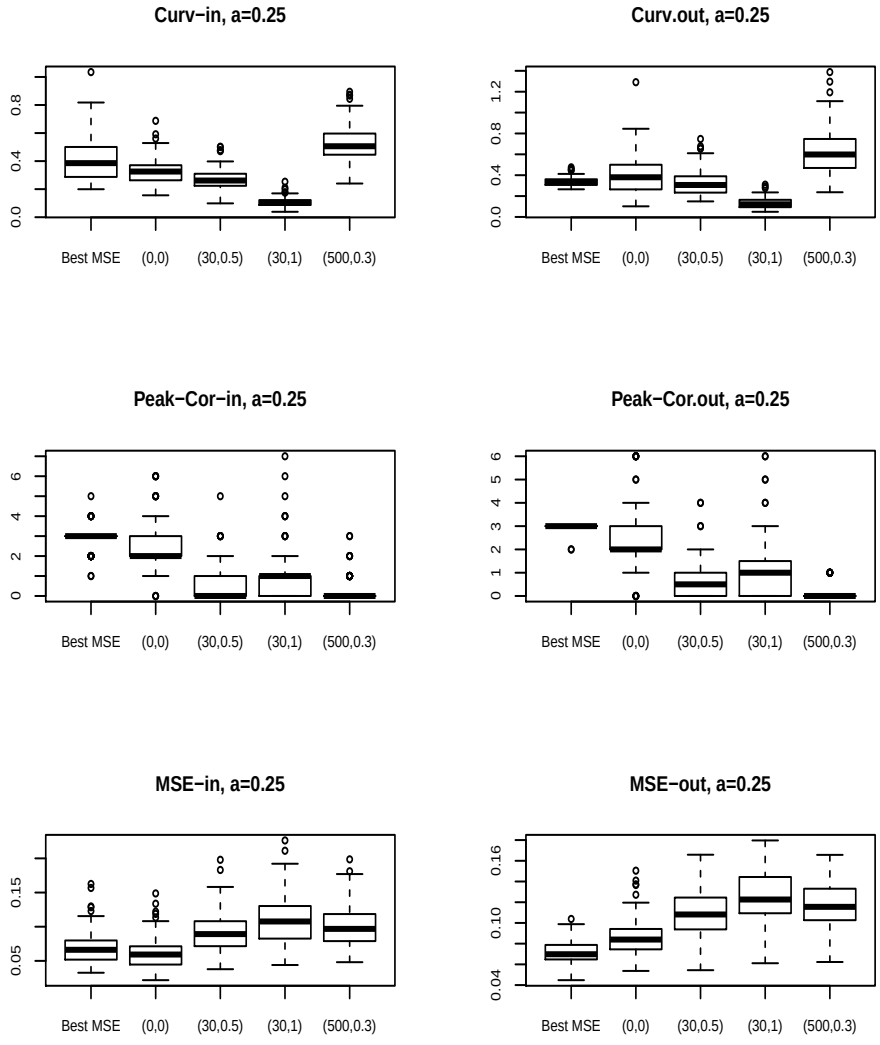

Figure 6: Empirical distributions of Curvature, Peak-Correlation and MSE based on periodogram: in-sample (left plots) and out-of-sample (right plots) for $a = 0.25$.

In order to illustrate the above results in visual terms we briefly compare outputs of the best benchmark filter (assuming knowledge of the DGP), of the balanced customized model-based filter (section 3.5) and of the nonparametric customized estimate (previous graphs) for a particular realization (the first of the sample); see Figure 7.

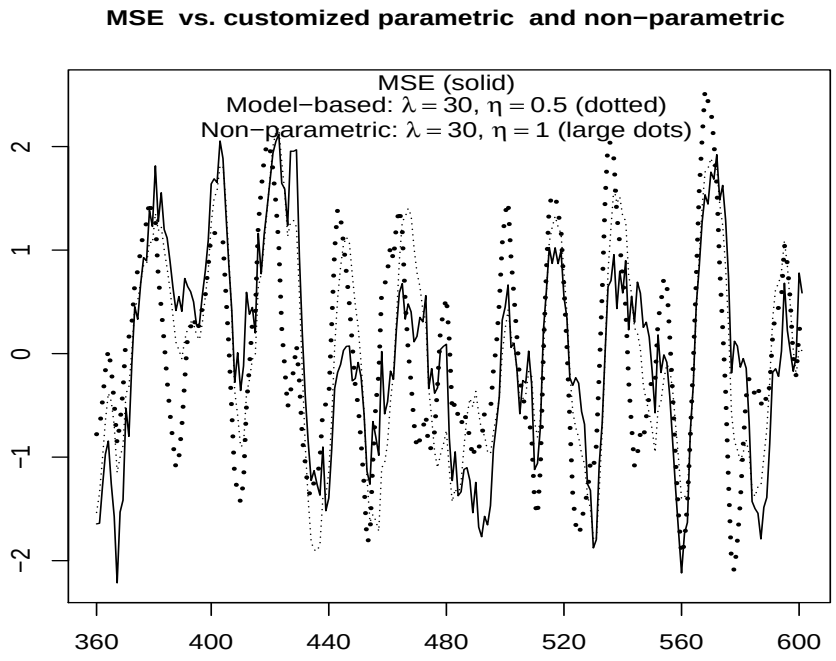

Figure 7: Outputs of best benchmark (solid), customized model-based (dotted) and customized nonparametric (large dots) filters, for a realization of an AR(1) process with $a = 0.25$.

The customized filter outputs lie to the left of the benchmark filter, and their appearance is smoother in the sense that noisy high-frequency ripples are damped more effectively.

5 Nowcasting Secular Growth in Indian Industrial Production

We analyze the Production of Total Industry in India[7], from April 1994 to Mai 2017, a monthly seasonally adjusted series shown in the top panel of Figure 8. Apparently, the secular growth of the series evolves over time. We propose to analyze this phenomenon by applying suitably parametrized concurrent filters to the monthly growth rates displayed in the bottom panel of Figure 8.

[7] `https://fred.stlouisfed.org/series/INDPROINDMISMEI`

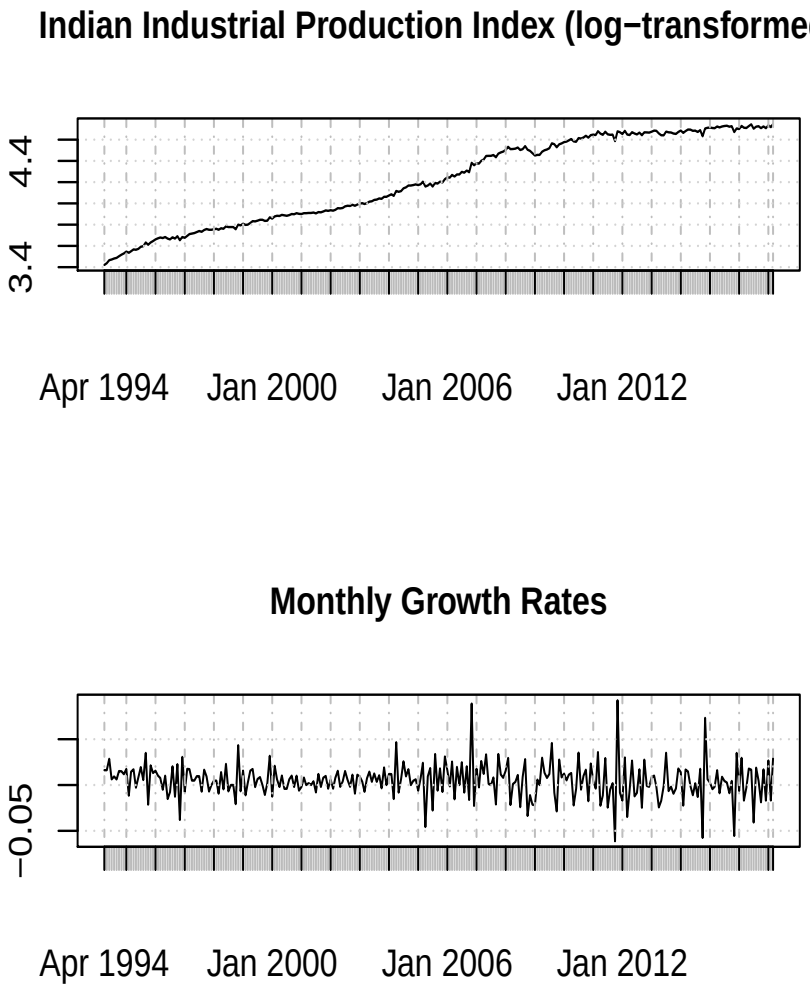

Figure 8: Indian industrial production index (monthly and seasonally adjusted).

5.1 Model-based Approach

Inspection of the autocorrelation plot in the top panel of Figure 9 reveals significant (negative) serial dependence in the growth rates at lags one and twelve, which is compatible with a model-based seasonal adjustment of the series (see McElroy (2012) for discussion). A SARIMA(0,0,1)(0,0,1) model provides an adequate description of the monthly growth rates. The resulting model-based spectral density

$$S(\omega_k) = |(1 - 0.34\exp(-i\omega_k))(1 - 0.22\exp(-i12\omega_k))|^2$$

is shown in the bottom panel of Figure 9.

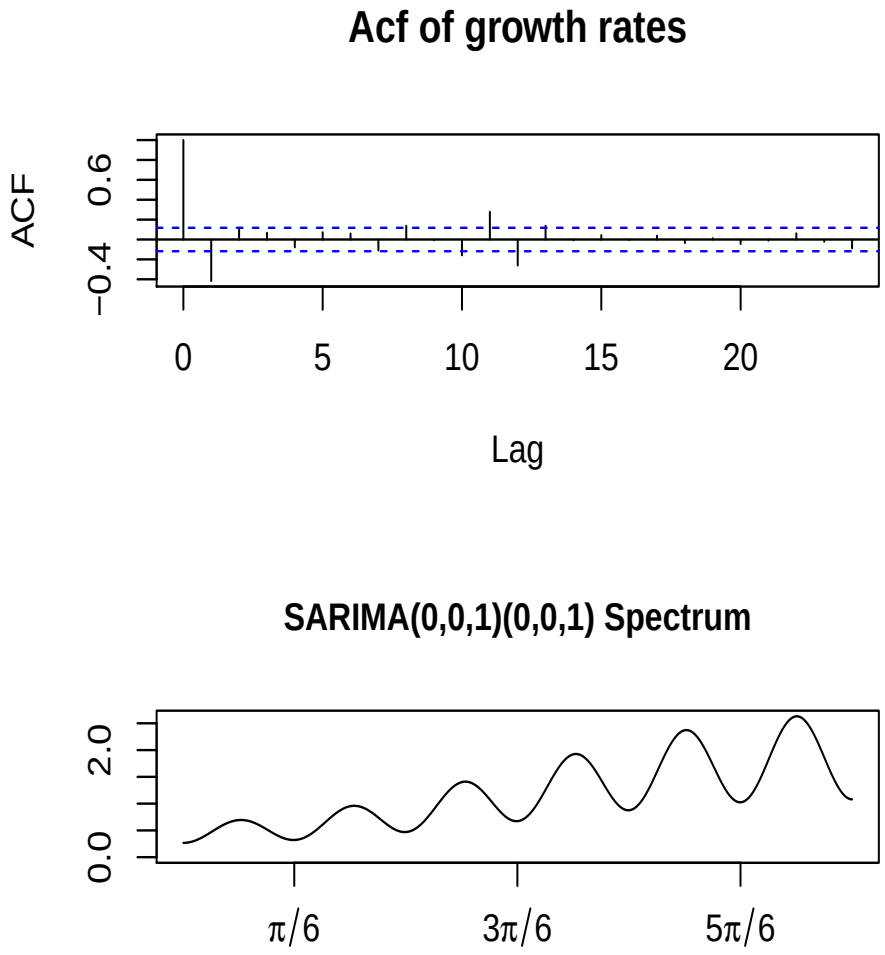

Figure 9: Indian industrial production index: acf of growth rates (top panel) and model-based spectrum (bottom panel).

In order to capture the long-term (secular) trend growth we apply an ideal lowpass filter with cutoff $\pi/72$, corresponding to a mean cycle duration of $2 * 72/12 = 12$ years. The amplitude function of the corresponding concurrent MSE filter is shown in Figure 10; note that the amplitude peaks at frequency 0.028, corresponding to a mean cycle duration of 9.2 years. This unusually tight specification allows extraction of the secular trend by smoothing-out the business-cycle.

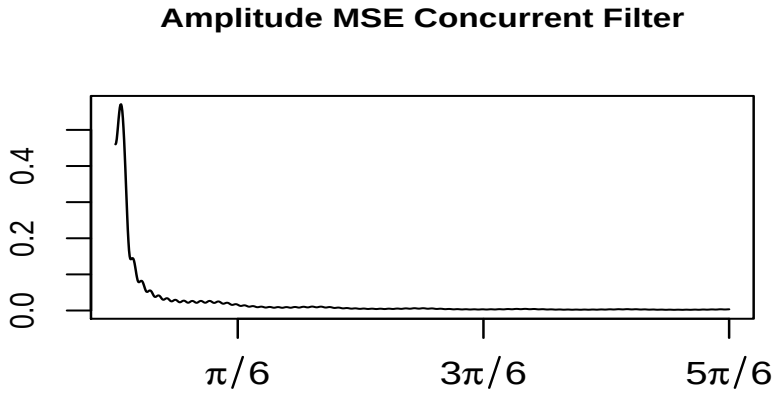

Figure 10: Amplitude function of concurrent MSE filter.

For sake of comparison, we benchmark performances against the simple exponential smoothing approach (Hyndman et al., 2008), which amounts to generating forecasts according to an ARIMA(0,1,1) model. (Double exponential smoothing corresponds to an ARIMA(0,2,2) model, and is unlikely to produce reasonable forecasts given that the data has already been differenced to stationarity.) The moving average parameter is obtained by fitting the model, and because the data is stationary the estimate is close to -1. (We also experimented with other fixed values of the moving average parameter, such as .8, .5, and .2; lower values correspond to forecasts that depend highly on the most current observation, and higher values generate forecasts that depend highly on the distant past. However, real-time performance was worse, so we present results using an estimated smoothing parameter.) With the sample extended by forecasting in this manner, the given target filter can be applied, with the resulting being a real-time signal extraction estimate generated by exponential smoothing.

5.2 Customization

In order to capture the long-term movements of industrial production, we require a real-time trend that is both smooth (so that we avoid false turning points) and timely. This objective is particularly important towards the end of the sample, where some interesting behavior occurs. To that end, we select $\lambda = 60$ and $\eta = 1$ in our design of a customized filter, thereby emphasizing Timeliness and Smoothness in the ATS-trilemma. Note that we rely on the above model-based spectrum for deriving both the MSE as well as the customized filters, whose corresponding outputs (rescaled for comparability) are displayed in Figure 11.

As expected, the customized filter output is smoother and lies to the left of the classic model-based design. The classic MSE filter has the broad swings (of period 12 years) that we hope a low-pass filter would provide, but is accompanied by many smaller movements, or noise, which locally can lead to the detection of spurious turning points. The customized real-time signal has all such high frequency noise eliminated (this is the contribution of the Smoothness term) while also preserving the chief low frequency swings (due to the presence of the Accuracy term in our criterion). Moreover, the customized real-time signal overall is more timely than the classic signal, and in the 2001 nadir leads by roughly a year.

In contrast, the signal from exponential smoothing is qualitatively similar to the classic real-time estimate in terms of Smoothness and Accuracy, but resembles the customized filter in terms

of Timeliness. Put another way, the customized real-time signal is a much smoother version of the signal from exponential smoothing. More interestingly, the customized filter reveals the presence of an up-turn starting in 2015, which indicates a possible relaxation of the zero-growth period towards the sample end. This feature of the series is missed by the classic MSE filter as well as by the simple exponential smoothing filter, whose outputs are subject to excessive lag and noise.

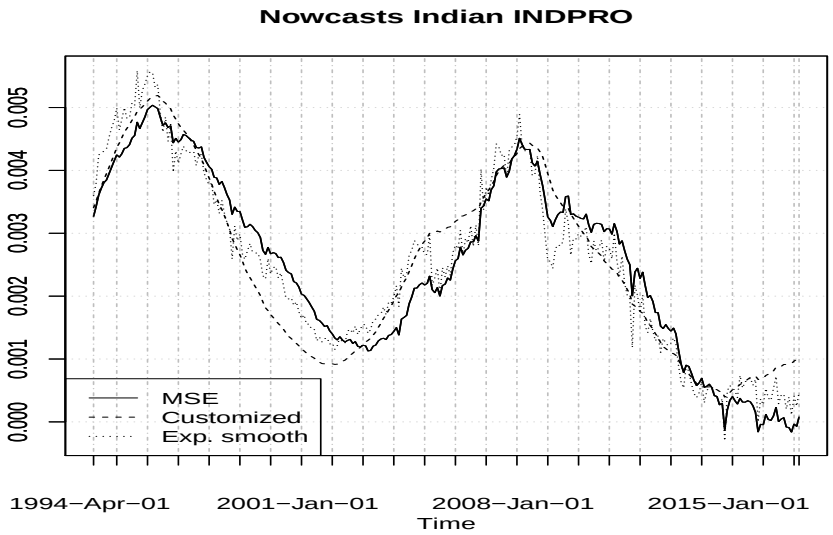

Figure 11: Concurrent filter outputs: classic MSE (solid) vs. simple exponential smoothing (dotted) vs. customized (shaded).

6 Summary

Real-time signal extraction is a difficult prospective estimation problem that involves linear combinations of (possibly infinitely many) multi-step ahead forecasts of a series. Addressing this problem directly with the DFA allows one to expand the forecast AT-dilemma into a richer ATS-trilemma. The resulting customized optimization criterion generalizes the classical MSE paradigm by allowing the user to utilize the customization triangle according to specific research priorities. In particular, Smoothness (Curvature) and Timeliness (Peak-Correlation) performances of a concurrent filter can be improved simultaneously, at the expense of Accuracy and total MSE.

The DFA and the ATS-trilemma are generic concepts, in the sense that they allow for arbitrary target signals or spectral estimates. In particular, classical ARIMA-based approaches can be replicated exactly, by supplying the corresponding entries. Once replicated, a particular approach can be customized to accommodate particular research priorities. Our numerical examples confirm that the best MSE filter, assuming knowledge of the true DGP, can be predictably outperformed in terms of Curvature and Peak-Correlation out-of-sample by suitably customized parametric (model-based) or nonparametric (periodogram) spectral estimates. When relying on the periodogram, overfitting may affect MSE performances as well as the customization effect, especially if the pass-band is short.

These techniques can be applied to real-time trend estimation, or nowcasting, of macroeconomic data, such as Gross Domestic Product or Industrial Production. Whereas larger economies, and in particular the economies of developed nations, tend to be stable (apart from times of crisis) and hence more easily forecastable, the economies of developing countries can be subject to many vicissitudes of policy or political instability. As a result, the detection of turning points in a timely fashion is extremely important; our analysis of Indian Industrial Production illustrates the utility

of filter customization, wherein we were able to simultaneously improve timeliness and smoothness of real-time estimates while preserving the overall signal features.

References

[1] Bell, W. and Hillmer, S. (1984) Issues involved with seasonal adjustment of economic time series. *J. Bus. Econ. Stat.* **2**, 291–320.

[2] Bell, W. and Martin, D. (2004) Computation of asymmetric signal extraction filters and mean squared error for ARIMA component models. *Journal of Time Series Analysis* **25**, 603–625.

[3] Brockwell, P. and Davis, R. (1991) *Time Series: Theory and Methods.* New York: Springer.

[4] Christiano, L. and Fitzgerald, T. (2003) The band pass filter. *International Economic Review* **44**, 435–465.

[5] Cleveland, W.P. (1972) *Analysis and Forecasting of Seasonal Time series.* PhD thesis, University of Wisconsin-Madison, 1972.

[6] Henderson, R. (1916) Note on graduation by adjusted average. *Trans. Actuar. Soc. Amer.* **17**, 43–48.

[7] Hodrick, R. and Prescott, E. (1997) Postwar U.S. business cycles: an empirical investigation. *Journal of Money, Credit, and Banking* **29**, 1–16.

[8] Hyndman, R., Koehler, A.B., Ord, J.K. and Snyder, R.D. (2008) *Forecasting with exponential smoothing: the state space approach.* Springer Science & Business Media.

[9] Koopman, S., Harvey, A., Doornik, J., and Shepherd, N. (2000) *Stamp 6.0: Structural Time Series Analyser, Modeller, and Predictor.* London: Timberlake Consultants.

[10] Maravall, A. and Caparello, G. (2004) Program TSW: Revised Reference Manual. Working paper 2004, Research Department, Bank of Spain. http://www.bde.es.

[11] McElroy, T. (2012) An Alternative Model-based Seasonal Adjustment that Reduces Over-Adjustment. *Taiwan Economic Forecast and Policy* **43**, 33–70.

[12] Wildi, M. and McElroy, T. (2016) Optimal Real-Time Filters for Linear Prediction Problems. *Journal of Time Series Econometrics* **8**(2), 155–192.

[13] Wildi M. (2005) *Signal Extraction: Efficient Estimation, Unit-Root Tests and Early Detection of Turning Points.* Lecture Notes in Economics and Mathematical Systems, 547, Springer.